

Dominant factors controlling glacial and interglacial variations in the treeline elevation in tropical Africa

Haibin Wu^{*†‡§}, Joël Guiot[†], Simon Brewer[†], Zhengtang Guo^{*†}, and Changhui Peng^{*§}

^{*}State Key Laboratory of Loess and Quaternary Geology, Institute of Earth Environment, Chinese Academy of Sciences, Xi'an 710075, China; [†]Centre Européen de Recherche et d'Enseignement des Géosciences de l'Environnement, Unité Mixte de Recherche 6635, Centre National de la Recherche Scientifique/Université Paul Cézanne, BP 80, 13545 Aix-en-Provence Cedex 4, France; [‡]Institute of Geology and Geophysics, Chinese Academy of Sciences, P.O. Box 9825, Beijing 100029, China; and [§]Institut des Sciences de l'Environnement, Département des Sciences Biologiques, Université du Québec à Montréal, Montréal, QC, Canada H3C 3P8

Edited by Zicheng Yu, Lehigh University, Bethlehem, PA, and accepted by the Editorial Board April 23, 2007 (received for review November 14, 2006).

The knowledge of tropical palaeoclimates is crucial for understanding global climate change, because it is a test bench for general circulation models that are ultimately used to predict future global warming. A longstanding issue concerning the last glacial maximum in the tropics is the discrepancy between the decrease in sea-surface temperatures reconstructed from marine proxies and the high-elevation decrease in land temperatures estimated from indicators of treeline elevation. In this study, an improved inverse vegetation modeling approach is used to quantitatively reconstruct palaeoclimate and to estimate the effects of different factors (temperature, precipitation, and atmospheric CO₂ concentration) on changes in treeline elevation based on a set of pollen data covering an altitudinal range from 100 to 3,140 m above sea level in Africa. We show that lowering of the African treeline during the last glacial maximum was primarily triggered by regional drying, especially at upper elevations, and was amplified by decreases in atmospheric CO₂ concentration and perhaps temperature. This contrasts with scenarios for the Holocene and future climates, in which the increase in treeline elevation will be dominated by temperature. Our results suggest that previous temperature changes inferred from tropical treeline shifts may have been overestimated for low-CO₂ glacial periods, because the limiting factors that control changes in treeline elevation differ between glacial and interglacial periods.

biome model | biome pollen scores | palaeoclimatology | pollen | vegetation model inversion

Pollen data show a lowering of treeline elevations during the last glacial maximum (LGM) by $\approx 1,000$ – $1,700$ m in mountains at a wide range of tropical and subtropical locations (1, 2). Assuming this decrease corresponds to a decrease in mean temperature and given a lapse rate of 5 – 6°C km^{-1} , this would imply a substantial cooling of ≈ 5 – 10°C in these areas, particularly at high elevations in the tropics (1, 2). However, a new faunal reconstruction of sea surface temperature (Multiproxy approach for the reconstruction of the glacial ocean surface: MARGO) for the tropics indicates a more limited cooling of $\approx 2^\circ\text{C}$ at low elevations during this period (3, 4), which is slightly more than the $\approx 1.5^\circ\text{C}$ estimated by using CLIMAP (5). These reconstructions are clearly not consistent, and although the differences could in principle be explained by a steeper atmospheric lapse rate, this parameter needs further validation by using more reliable data (6–8). Nonetheless, this lack of agreement leaves considerable uncertainty about what the tropical climate was really like during the last ice age.

Physiological data and models have demonstrated that the processes that modify carbon and water uptake in plants are highly dependent on CO₂ concentrations (9, 10). This suggests that modern plant–climate relationships are not representative of interactions between plants and climate in the past (9–11), because the atmospheric CO₂ concentration has fluctuated significantly between glacial and interglacial periods (12). Furthermore, simulations using vegetation models by

Jolly and Haxeltine (13) have shown that low atmospheric CO₂ concentration could by itself cause the observed replacement of tropical mountain forests by scrub in Africa during the LGM. In the same way, palaeoecological $\delta^{13}\text{C}$ data from Africa (14) also reveal that the lower atmospheric CO₂ concentration during the LGM could have contributed to the decreased elevation of alpine treelines. These studies suggest that previous pollen-based estimates of temperature decreases during the LGM may have been overestimated. A modeling approach combined with appropriate data is thus necessary to understand these discrepancies (15, 16).

In this paper, we describe our use of an improved inverse vegetation modeling approach (17) by a physiological process-based vegetation model, BIOME4 (18), in an inverse mode (15), and the BIOME6000 pollen data (19) to examine how changes in atmospheric CO₂ concentration and climate might account for the observed distribution of African mountain vegetation during the LGM.

Results

We applied the improved model version (17) to modern pollen samples to validate the approach by reconstructing the modern climate at each site and comparing it with observed values. High correlation coefficients (Table 1), intercepts close to 0 (with the exception of mean temperature of the warmest month and growing degree days $>5^\circ\text{C}$), and slopes close to 1 (with the exception of mean temperature of the coldest month) demonstrated that the inversion method worked well for most variables and confirmed that the climate signals contained in the modern pollen data could be quantitatively extracted by means of the inverse vegetation modeling method. These results confirm the reliability of the LGM climate and biome reconstructions.

During the LGM, the inverse vegetation model successfully simulated the biome at all pollen collection sites. The results show that the change in the mean annual temperature generally varied from 1 to -3°C and averaged $\approx 2^\circ\text{C}$ lower than the modern value in the tropics but with large error bars (Fig. 1A). Annual precipitation decreased by between 200 and $1,000 \text{ mm}\cdot\text{yr}^{-1}$ relative to the present for equatorial regions (Fig. 1B), and the robust relationship between the percentage change in precipitation and elevation in tropical Africa (Fig.

Author contributions: H.W. and J.G. designed research; H.W. performed research; H.W. and J.G. contributed new reagents/analytic tools; H.W., J.G., S.B., Z.G., and C.P. analyzed data; and H.W., J.G., S.B., Z.G., and C.P. wrote the paper.

The authors declare no conflict of interest.

This article is a PNAS Direct Submission. Z.Y. is a guest editor invited by the Editorial Board.

Abbreviations: LGM, last glacial maximum; NPP, net primary production; E_n , experiment n ; asl, above sea level; ppmv, parts per million volume.

[§]To whom correspondence may be addressed. E-mail: haibin.wu2001@yahoo.com or peng.changhui@uqam.ca.

This article contains supporting information online at www.pnas.org/cgi/content/full/0610109104/DC1.

© 2007 by The National Academy of Sciences of the USA

Table 1. Regression coefficients between the reconstructed climates for Africa using the inverse vegetation model and the observed meteorological values

Climate proxy	Slope	Intercept	R	ME	RMSE
Mean annual temperature	0.92 ± 0.02	3.43 ± 0.45	0.88	1.72	2.46
Mean temperature of the coldest month	0.80 ± 0.02	2.54 ± 0.45	0.82	-1.35	3.23
Mean temperature of the warmest month	0.88 ± 0.02	6.75 ± 0.51	0.87	3.67	2.47
Total annual precipitation	1.11 ± 0.02	-21.99 ± 27.66	0.90	98.25	324.06
Precipitation in January	1.11 ± 0.01	-3.12 ± 1.39	0.96	7.62	26.84
Precipitation in July	1.07 ± 0.02	2.50 ± 2.65	0.92	8.82	43.06
Growing degree-days above 5°C	0.92 ± 0.02	$1,131.59 \pm 128.21$	0.89	634.86	897.17
Ratio of actual to potential evapotranspiration	0.93 ± 0.03	2.35 ± 1.62	0.81	-1.49	10.21

R, correlation coefficient (\pm standard error); ME, mean value of the residuals; RMSE, rms error. These values are calculated based on 585 observations.

1C) suggests that the changes depended strongly on elevation: the rainfall decrease was greatest at the highest elevations.

A sensitivity analysis was performed to identify the dominant factors controlling the observed changes in treeline elevation (Fig. 2). When temperature is increased from its LGM reconstruction to its modern value, and precipitation and CO₂ are kept at their LGM values [see experiment 1 (E1) in *Materials and Methods*], a change in vegetation from steppe (STEP) to mountain forest (WAMX) is seen at only one site above the LGM treeline elevation (Fig. 2B and C), suggesting that temperature played a relatively limited role in controlling the treeline shift. When precipitation (E2) and atmospheric CO₂ concentration (E3) change from their reconstructed LGM value to their modern values, and the other variables are fixed at their LGM values, the biome at most of the pollen sites changes from nonforest biomes to forest biomes (Fig. 2D and E), in good agreement with modern observations (20) (Fig. 2A). These last two variables, therefore, seem to be at least partially responsible for explaining the treeline shift.

To further estimate the relative importance of atmospheric CO₂ and precipitation on treeline changes, we explored the parameter space between the LGM values and modern values for precipitation and CO₂ concentration (E4) by using steps of 7% and 10 parts per million volume (ppmv), respectively. For each combination of variables, we plotted the simulated treeline elevation (Fig. 3A). Fig. 3A shows that the treeline elevation changes more quickly in response to changes in precipitation than to changes in atmospheric CO₂ during the period from the LGM to the beginning of the Holocene [at 270 ppmv CO₂ concentration (12)], and that the effect of precip-

itation is approximately one to three times the magnitude of the change with respect to CO₂ in the altitude range from $\approx 1,800$ to 3,000 m above sea level (asl) (Fig. 3B). This shows that precipitation exerted a stronger control on the change in treeline elevation than the atmospheric CO₂ level.

From the start of the Holocene to modern times, treeline elevation no longer significantly depends on changes in precipitation and atmospheric CO₂, especially at CO₂ concentrations >300 ppmv (Fig. 3A), suggesting that these two factors no longer act as limits. To identify the most important factor responsible for treeline changes during this period, the sensitivity of elevation between the start of the Holocene and the modern period was explored as a function of changes in temperature, precipitation, and atmospheric CO₂ (E5) to extract any information that might have been missed in E4 when temperature was kept at the LGM level. Fig. 3C shows that the increase in treeline elevation responded most strongly to temperature increases and was not sensitive to changes in precipitation and atmospheric CO₂ above $\approx 3,000$ m asl altitude. We obtained similar results for the predicted future scenario (sites from ref. 21) (E6, Fig. 3C). Under that scenario, temperature will play the dominant role in the treeline shift. This can be explained by the fact that water and carbon are sufficiently available during these periods so they are not limiting. These factors thus play a secondary role in determining the forest vegetation in mountainous areas of the tropics.

Discussion

Previous estimates of the LGM climate in tropical Africa are based on the modern observation that temperature is a limiting

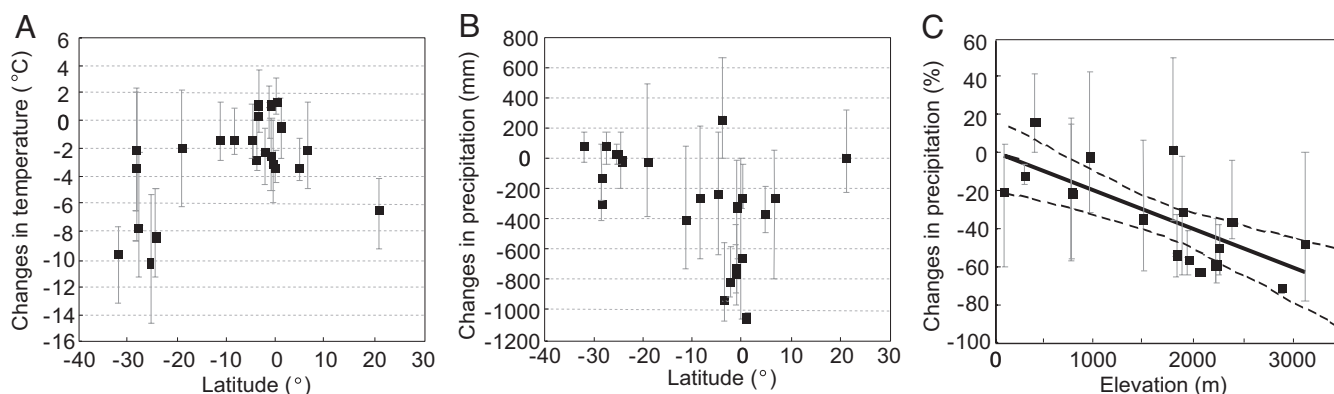


Fig. 1. Reconstructed temperature and precipitation changes in Africa as a function of latitude and elevation during the LGM. The values are expressed as deviations from modern mean values, and error bars represent 95% confidence intervals. (A) Mean annual temperature as a function of latitude. (B) Total annual precipitation as a function of latitude. (C) Total annual precipitation changes as a function of elevation in tropical regions ($23.5^{\circ}\text{S} < \text{latitude} < 23.5^{\circ}\text{N}$). The solid line represents the least-squares linear regression. Dashed lines are the upper and lower 95% confidence limits, respectively. The linear relationship is defined as: Deviation in total annual precipitation (%) = $-0.020(\pm 0.005)$ Elevation - $0.727(\pm 8.861)$; $R^2 = 0.540$, $n = 17$, $P = 0.0007$.

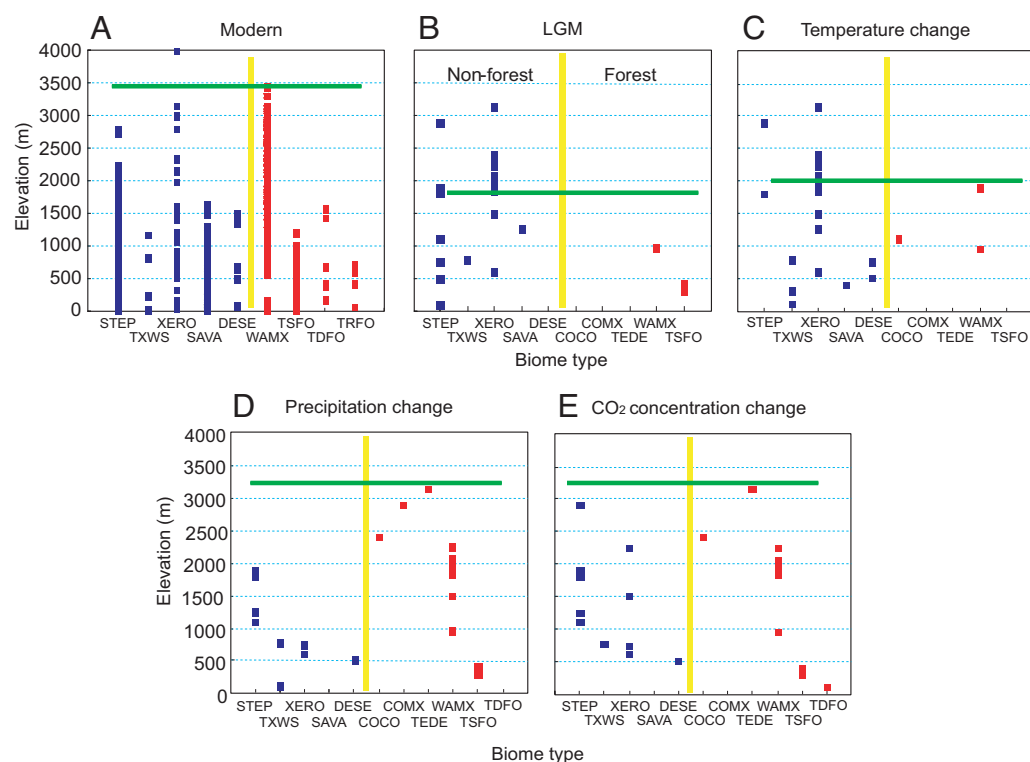


Fig. 2. Effects of temperature, precipitation, and atmospheric CO_2 concentration on treeline changes in Africa from the LGM to the modern period. **A** and **B** are the observed pollen biome distributions as a function of elevation during the modern period and during the LGM. **C–E** are simulated biome distributions at LGM sites with, respectively, increasing temperature (E1), precipitation (E2), and atmospheric CO_2 concentration (E3) from the LGM to the present. The yellow bar separates the nonforest biomes (left) from the forest biomes (right). The green line is the elevation of the treeline, which was determined by drawing a horizontal line at the maximum elevation of forest biomes whose NPP is $>300 \text{ g C m}^{-2} \text{ yr}^{-1}$ (13). The maximum elevation ($\approx 3,500 \text{ m}$) for modern pollen biomes (**A**) is in agreement with the observed modern forest limit, which occurs between $\approx 3,000$ and $3,450 \text{ m}$ in Africa (20). The LGM treeline elevation was reconstructed based on the pollen spectra at $1,778 \text{ m}$, because it contains high pollen abundances for several woody taxa (i.e., *Macaranga*, *Podocarpus*, *Olea*, and *Syzygium*), and its second pollen biome score was the forest biome (WAMX). Biomes: COCO, cool coniferous forest; COMX, cool mixed forest; DESE, desert; SAVA, savanna; STEP, steppe; TDFO, tropical dry forest; TEDE, temperate deciduous forest; TRFO, tropical rain forest; TSFO, tropical seasonal forest; TXWS, tropical xerophytic woods/scrub; WAMX, broadleaved evergreen/warm mixed forest; XERO, xerophytic woods/scrub. The list of biomes for Fig. 2A is different from that for Fig. 2B–E.

factor for treeline elevation (2, 22). The temperature decrease compared with the modern value is broadly consistent with the results obtained by using the BIOME3 model (a decrease of $\approx 6^\circ\text{C}$) (13) if the change in biome is attributed to temperature alone. In the present study, the cooling of $\approx 2^\circ\text{C}$ based on inverse vegetation modeling is obviously less than previous estimates, because the improved method allows us to separate out the effects of changes in temperature, precipitation, and atmospheric CO_2 on biome distributions. Other climate reconstructions based on a best-analogue method that can account for the effect of a decrease in precipitation of $\approx 30\%$ show a modest reduction in temperature of $\approx 3\text{--}4^\circ\text{C}$ (23, 24). These estimates are closer to our results, because they take into account a range of values for temperature and precipitation, but they neglect the effects of CO_2 concentration. Our results are consistent with the results of recent MARGO reconstructions of sea surface temperature ($\approx 1\text{--}3^\circ\text{C}$ of cooling) in the tropics (3, 4), and with simulations for tropical oceans ($\approx 0.8\text{--}3.5^\circ\text{C}$ decrease) by using atmospheric general circulation models (8, 25). The dryer-than-present condition, at least qualitatively, is in agreement with the East African lake-level variations reexamined by Barker and Gasse (26).

Another important result of our study is that the lowering of the treeline elevation that occurred during the LGM appears to have been triggered primarily by a dryer-than-normal period throughout the region, with the lower atmospheric concentration of CO_2 playing a lesser but important role. This can be explained by two facts: the environment was more

water-limited during the LGM than at present in tropical Africa (26), and lower concentrations of CO_2 amplify the effect of an arid climate on plants through their effects on leaf conductance and water-use efficiency (9, 10).

Although the contribution of CO_2 fertilization to terrestrial ecosystems has been uncertain based on currently available data (27), Cowling and Field (28) have observed a good fit between modeled and observed response of LAI to changes in low CO_2 for BIOME3, and the predictions of net primary production (NPP) response to CO_2 fertilization in the future by using the Lund–Postdam–Jena (LPJ) model (29) is also in agreement with experimental evidence by Norby *et al.* (27). Because the treatment of CO_2 fertilization in BIOME3 and LPJ is same as BIOME4, these comparisons indicate that BIOME4 model can realistically predict the response to the CO_2 fertilization.

Various lines of evidence from fossil pollen (2, 14, 24, 30) support these results. The most characteristic feature of the treeline change due to the LGM is that the expansion of moist montane forest occurred at different rates and times in different tropical areas (14, 24, 30). This indicates the importance of regional climate in controlling the treeline, as opposed to the role of atmospheric CO_2 , which would lead globally to a gradual and synchronous increase in the treeline elevation that followed the change in atmospheric CO_2 concentration. Furthermore, pollen analysis shows a well developed forest belt in the Central East African mountains at an elevation of $\approx 2,000\text{--}2,400 \text{ m}$ during the last glacial period between 30 and

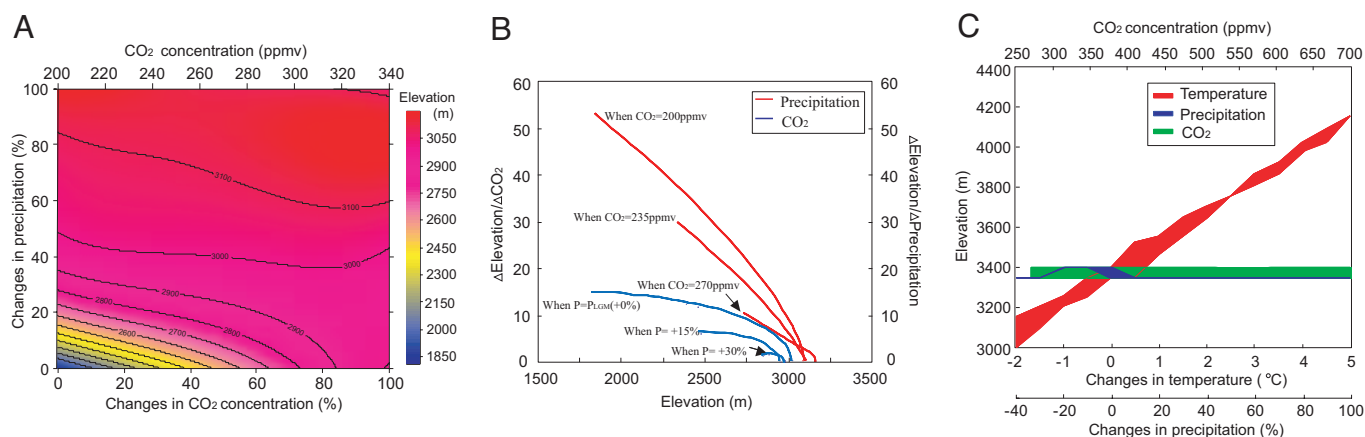


Fig. 3. Sensitivity analysis for the response of treeline elevation in tropical Africa to changes in atmospheric CO₂ concentration and precipitation from the LGM to future. (A) Changes in treeline elevation simulated as a function of changes in precipitation (y axis) and changes in atmospheric CO₂ concentration (x axis) from the LGM to the modern period (E4). A surface was fitted by using a fourth-order polynomial regression. Numbered lines are the isoline for treeline elevation. Precipitation and CO₂ concentration are expressed as percentage changes from the LGM (0%) to the modern period (100%). (B) Changes in the ratio between $\Delta\text{Elevation}/\Delta\text{precipitation}$ and $\Delta\text{Elevation}/\Delta\text{CO}_2$ in function of treeline elevation from the LGM to present. The relations were calculated under 200, 235, and 270 ppmv CO₂ concentrations for $\Delta\text{Elevation}/\Delta\text{precipitation}$ (red line), and under increasing of 0%, 15%, and 30% precipitation conditions for $\Delta\text{Elevation}/\Delta\text{CO}_2$ (blue line). (C) Changes in treeline elevation as a function of changes in temperature, precipitation, and CO₂ concentration from the start of the Holocene to future. In the left side of the graph, all values between the start of the Holocene and the modern period (E5) were investigated. In the right side of the graph, all values were simulated between the modern value and the future (E6). The analysis used 36 sites at intervals of 50–100 m in the Kenya Mountain area (latitudes of 0.20°S–0.12°S, longitudes of 37.22°E–37.45°E, and elevations of 3,001–4,993 m) to investigate changes in treeline elevation by using the database of the Global Land One-Kilometre Base Elevation Project (21). Simulations were performed across the range of values with a step of 10%. The red line shows the changes in treeline elevation as a function of temperature for all values of precipitation and atmospheric CO₂ concentration between the start of the Holocene and future conditions. The blue line shows changes in treeline elevation as a function of precipitation for all values of atmospheric CO₂ concentration from the start of the Holocene to the future but with temperature remaining at modern values. The green line shows the changes in treeline elevation as a function of CO₂ concentration for all values of precipitation from the start of the Holocene to the future but with temperature remaining at modern values.

40 kyBP, whereas this vegetation was replaced by nonforest biomes during the LGM (2, 24, 30). This evidence also does not support the view that atmospheric CO₂ was a dominant limiting factor in determining treeline elevation, because the atmospheric CO₂ concentration was similar during both periods (12).

Under the Holocene, modern, and future scenarios, sensitivity analysis revealed that the increased elevation of tropical mountain treelines was mainly controlled by temperature. This is in good agreement with the observation that the presence or absence of trees at treeline under modern conditions is determined by physiological limits at low temperatures (22). The dominant role of temperature on tree growth has also been well established for warm and cool periods of the Holocene (31). In the past century, the increasingly warm climate has had a substantial influence on shifts in the treeline in the tropics (32) as well as in other regions of the world (33).

Our results indicate that the limiting factors that control changes in the elevation of the African treeline differ between glacial and interglacial periods. Thus, previous estimates of tropical cooling during the LGM period based on the assumption that treeline depends on temperature seem unrealistic. Because greenhouse gases have been one major factor affecting tropical temperature at the LGM, the magnitude of the tropical cooling during the period has an important implication for Earth's system sensitivity to changes in atmospheric CO₂ as simulated by general circulation models (34). Our relatively moderate cooling of $\approx 2^\circ\text{C}$ in the tropics suggests that the earth system is at the moderate side of the range of CO₂ sensitivity, at least past atmospheric CO₂ forcing.

Materials and Methods

The BIOME6000 project (19) has gathered global pollen data for three periods: modern, $6,000 \pm 500$ kyBP, and $21,000 \pm 2,000$ kyBP. Each pollen assemblage has been transformed into biome

scores according to its affinity with a set of predefined biomes and was assigned to the most likely biome. The modern data set (35) includes 629 pollen spectra in Africa and was used in the present study to validate the method for more ancient periods. The LGM data set (35) contains 23 data sites covering an altitudinal range from 100 to 3,140 m asl.

We used a recent version of BIOME4 (18) and an inversion technique (15) to estimate climate based on BIOME6000 pollen data. The principle behind this method [see [supporting information \(SI\) Text](#)] is that we can attempt to estimate the inputs for the vegetation model (i.e., the climate) if we have information related to the output of the model (i.e., biome scores at pollen collection sites). BIOME4 is especially improved in comparison with BIOME3 (36) with respect to arctic vegetation, and this is an important advantage of the newer model for the simulation of LGM vegetation at high elevations in the tropics. However, the biome typology used by BIOME4 is not fully compatible with the biome typology of the pollen data. We thus defined a transfer matrix to match the BIOME4 typology to the pollen typology (see [SI Table 3](#)) that was qualitatively obtained by examination of the modern pollen biome score data and modern vegetation maps. This was done as an alternative to develop an NPP to pollen production relationship based on an artificial neural network between modern pollen-derived plant functional types (PFT) scores and simulated NPP values of the PFT (15). This transfer matrix is less susceptible than the relationship by Guiot *et al.* (15) to being affected by a strong human perturbation of the modern biomes at pollen collection sites.

To identify the dominant factors controlling the changes in African treeline elevation, six experiments were carried out. E1, temperature changed from the LGM value to the modern value, but precipitation and CO₂ remained at their respective LGM values [CO₂ = 200 ppmv for LGM (12)]. E2, precipitation changed from the LGM value to the modern value, but

temperature and CO₂ remained at their respective LGM values. E3, CO₂ concentration changed from 200 (LGM) to 340 ppmv (modern, because the modern pollen samples were collected in 1970s) (37), but temperature and precipitation remained at their respective LGM values. E4, all values between the LGM and the modern values were investigated for CO₂ concentration and precipitation, but temperature remained at LGM values. E5, all values between the start of the Holocene and the modern period were investigated for CO₂ concentrations ranging from 270 (12) to 340 ppmv, temperatures ranging from −2°C below to +2°C above modern values, and precipitation ranging from −40% below to +40% above modern values. E6, all values were simulated between the modern value and the future, with CO₂ concentration, tem-

perature, and precipitation ranging (respectively) from 340 to 700 ppmv, +0 to +5°C above the modern value, and precipitation +0 to +100% above the modern value.

We thank the editor, Zicheng Yu, and James P. Kennett for constructive suggestions that greatly improved this manuscript. This research was supported by funding from the European Union Environment, Sustainable Development Program (project MOTIF: EVK2-CT-2002-00153), the National Natural Science Foundation of China (Grants 40302021 and 40231001), the National Basic Research Program of China (Grant 2004CB720203), the Chinese Academy of Sciences (Grant KZCX3-SW-139), a grant from the French Ministry of Research (W.H.), as well as the Canada Research Chair Program and Natural Sciences and Engineering Research Council Discover Grant.

1. Rind D, Peteet D (1985) *Q Res* 24:1–22.
2. Flenley JR (1998) *Clim Change* 39:177–197.
3. Barrows TT, Juggins S (2005) *Q Sci Rev* 24:1017–1047.
4. Kucera M, Weinelt M, Kiefer T, Pflaumann U, Hayes A, Weinelt M, Chen MT, Mix AC, Barrows TT, Cortijo E, *et al.* (2005) *Q Sci Rev* 24:951–998.
5. CLIMAP Project Members (1981) Seasonal Reconstructions of the Earth's Surface at the Last Glacial Maximum. Geological Society of American Map and Chart Series, MS-36 (Geological Society of America, Boulder, CO).
6. Rind D (1990) *Nature* 346:317–318.
7. Farrera I, Harrison SP, Prentice IC, Ramstein G, Guiot J, Bartlein PJ, Bonnefille R, Bush M, Cramer W, von Grafenstein U, *et al.* (1999) *Clim Dyn* 15:823–856.
8. Pinot S, Ramstein G, Harrison SP, Prentice IC, Guiot J, Stute M, Joussaume S (1999) *Clim Dyn* 15:857–874.
9. Polley HW, Johnson HB, Marinot BD, Mayeux HS (1993) *Nature* 361:61–64.
10. Cowling SA, Sykes MT (1999) *Q Res* 52:237–242.
11. Boom A, Mora G, Cleef AM, Hooghiemstra H (2001) *Rev Palaeobot Palynol* 115:147–160.
12. Siegenthaler U, Stocher TF, Monnion E, Luthi D, Schwander J, Stauffer B, Raynaud D, Barnola JM, Fischer H, Masson-Delmotte V, *et al.* (2005) *Science* 310:1313–1317.
13. Jolly D, Haxeltine A (1997) *Science* 276:786–788.
14. Street-Perrott FA, Huang YS, Perrott RA, Eglinton G, Barker P, Khelifa LB, Harkness DD, Olago DO (1997) *Science* 278:1422–1426.
15. Guiot J, Torre F, Jolly D, Peyron O, Boreux JJ, Cheddadi R (2000) *Ecol Model* 127:119–140.
16. Williams JW, Webb T, III, Shurman BN, Bartlein PJ (2000) *Q Res* 53:402–404.
17. Wu HB, Guiot J, Brewer S, Guo ZT (2007) *Clim Dyn*, in press.
18. Kaplan JO, Bigelow NH, Prentice IC, Harrison SP, Bartlein PJ, Christensen TR, Cramer W, Matveyeva NV, McGuire AD, Murray DF, *et al.* (2003) *J. Geophys Res* 108:8171–8187.
19. Prentice IC, Jolly D, BIOME 6000 P (2000) *J Biogeogr* 27:507–519.
20. Bussmann RW (2006) *Lyonia* 11:41–66.
21. *The Global Land One-Kilometre Base Elevation Project* (1999), www.ngdc.noaa.gov/mgg/topo/globe.html, Ver. 1.0.
22. Körner C, Paulsen J (2004) *J Biogeogr* 31:713–732.
23. Bonnefille R, Roeland JC, Guiot J (1990) *Nature* 346:347–349.
24. Bonnefille R, Chalié F (2000) *Global Planet Change* 26:25–50.
25. Shin SI, Liu Z, Otto-Bliesner B, Brady EC, Kutzbach JE, Harrison SP (2003) *Clim Dyn* 20:127–151.
26. Barker P, Gasse F (2003) *Q Sci Rev* 22:823–837.
27. Norby RJ, DeLucia EH, Gielen B, Calfapietra C, Giardina CP, King JS, Ledford J, McCarthy HR, Moore DJP, Ceulemans R, *et al.* (2005) *Proc Natl Acad Sci USA* 102:18052–18056.
28. Cowling SA, Field CB (2003) *Global Biogeochem Cycl* 17:1007–1020.
29. Cramer W, Bondeau A, Woodward FI, Prentice IC, Betts RA, Brovkin V, Cox PM, Fisher V, Foley JA, Friend AD, *et al.* (2001) *Global Change Biol* 7:357–373.
30. Taylor DM (1990) *Palaeogeogr Palaeoclimatol Palaeoecol* 80:283–300.
31. Heiri C, Bugmann H, Tinner W, Heiri O, Lischke H (2006) *J Ecol* 94:206–216.
32. Shugart, H. H. French NHF, Kasischke ES, Slawski JJ, Dull CW, Shuchman RA, Mwangi J (2001) *Global Change Biol* 7:247–252.
33. Walthers GR (2003) *Persp Plant Ecol Evol Syst* 6:169–185.
34. Ruddiman WF (2000) in *Earth's Climate: Past and Future* (Freeman, New York), pp 405–422.
35. Elenga H, Peyron O, Bonnefille R, Jolly D, Cheddadi R, Guiot J, Andrieu V, Bottema S, Buchet G, de Beaulieu JL, *et al.* (2000) *J Biogeogr* 27:621–634.
36. Haxeltine A, Prentice IC (1996) *Global Biogeochem Cycles* 10:693–709.
37. Friedli H, Löffler H, Oeschger H, Siegenthaler U, Stauffer B (1986) *Nature* 324:237–238.